Communications in Statistics—Simulation and Computation®, 43: 761–776, 2014

ISSN: 0361-0918 print / 1532-4141 online
DOI: 10.1080/03610918.2012.714033

Taylor & Francis
Taylor & Francis Group

Control Charts for Monitoring Burr Type-X Percentiles

Y. L. LIO,[1] TZONG-RU TSAI,[2] M. ASLAM,[3] AND NAN JIANG[1]

[1]Department of Mathematical Sciences, University of South Dakota, Vermillion, SD, USA
[2]Department of Statistics, Tamkang University, New Taipei City, Taiwan
[3]Department of Statistics, Forman Christian College University, Lahore, Pakistan

When the sampling distribution of a parameter estimator is unknown, using normality asymptotically, the Shewhart-type chart may provide improper control limits. To monitor Burr type-X percentiles, two parametric bootstrap charts (PBCs) are proposed and compared with the Shewhart-type chart via a Monte Carlo simulation. Simulation results exhibit that the proposed PBCs perform well with a short average run length to signal out-of-control when the process is out-of-control, and have more adequate control limits than the Shewhart-type chart in view of in-control false alarm rate. An example regarding single fiber strength is presented for illustrating the proposed PBCs.

Keywords Average run length; Control charts; False alarm rate; Parametric bootstrap; Percentile; Shewhart chart.

Mathematics Subject Classification Primary 62F40; secondary 62P30.

1. Introduction

Burr (1942) was the pioneer to introduce the Burr type-X (BTX) distribution in the literature. Since then, the BTX distribution has received special attention in reliability study and failure time modeling. The cumulative distribution function (CDF) of the BTX distribution can be defined as follows:

$$F(t;\alpha,\lambda) = \left(1 - e^{-(\lambda t)^2}\right)^{\alpha}, \quad t > 0, \tag{1}$$

where $\alpha > 0$ and $\lambda > 0$ are shape and scale parameters, respectively. The BTX distribution of Eq. (1) is a generalized Rayleigh distribution with no shift parameter and a special distribution of the exponentiated Weibull distribution, which was introduced by Mudholkar and Srivastava (1993, 1995). Many aspects of the BTX distribution had been studied by Sartawi and Abu-Salih (1991), Ahmad et al. (1997), Jaheen (1995, 1996), Kundu and Raqab (2005), Raqab (1998), and Surles and Padgett (1998, 2001).

In many industrial applications, a specific quality condition of the product's lifetime is often required for engineering design consideration. Surles and Padgett (2001) observed that the BTX distribution could be used quite effectively in modeling strength data as

Received March 25, 2012; Accepted July 16, 2012
Address correspondence to Yuhlong Lio, PhD, Department of Mathematical Sciences, University of South Dakota, 414 East Clark Street, Vermillion, 57069 USA; E-mail: Yuhlong.lio@usd.edu

well as modeling general lifetime data. However, to our best knowledge, no control charts for monitoring BTX lifetime percentiles have been presented in the literature, yet. The well-known Shewhart-type control chart is constructed based on the assumption that data come from a near-normal distribution. Although the sampling distribution of the maximum likelihood estimator of the BTX percentile can be shown as a normal distribution, asymptotically, the exact sampling distribution of the maximum likelihood estimator of a BTX percentile is unknown. In this case, the Shewhart-type control chart using a finite subgroup size may not provide appropriate control limits. Therefore, computer-based methods such as bootstrap methods could be good candidates to establish the control limits for monitoring BTX percentiles. Efron and Tibshirani (1993), Gunter (1992), and Young (1994) provided comprehensive discussions of bootstrap techniques.

Bootstrap methods are helpful to establish control chart limits when the sampling distribution of a parameter estimator is not available. Many authors have studied the constructions of bootstrap charts. Bajgier (1992) developed a bootstrap chart to monitor the process mean, which was a competitor to the Shewhart $\overline{X}$ chart. However, if all pre-samples were not in control, the bootstrap chart could become conservative due to producing too wide control limits, regardless of the underlying distribution of the process variable. Many referred articles, such as Jones and Woodall (1998), Liu and Tang (1996), and Seppala et al. (1995), had pointed out that bootstrap charts could alarm for out-of-control status quicker than the Shewhart-type chart could if the underlying distribution of process variable was skewed. An advantage of bootstrap method is to release the restriction from the theoretical sampling distribution of an estimator. The computation time of a bootstrap method is perhaps a perceived disadvantage, but actually is not, considering today's computer power availability. Based on the advent of modern powerful and accessible computers, any simulation-based estimation can be more easily implemented to obtain computation results in an affordable amount of time.

Nichols and Padgett (2005) developed a parametric bootstrap chart (PBC) based on Weibull distribution for monitoring the tensile strength percentile in the production process of carbon fiber. They found that the PBC could alarm for an out-of-control process quicker than the Shewhart-type chart, proposed by Padgett and Spurrier (1990). Lio and Park (2008) investigated PBCs for Birnbaum-Saunders percentiles based on maximum likelihood estimation method and moment method. According to their simulation results, they found that both bootstrap charts provided a shorter average run length (ARL) when the process was shifted to out-of-control. Lio and Park (2010) studied PBCs for inverse Gaussian percentiles and showed that the bootstrap charts performed better than the percentile control chart using Bonferroni bounds, which was provided by Onar and Padgett (2000). The bootstrap method only uses bootstrap samples, which are generated by using a sample data of an estimator, to generate the sampling distribution of the estimator, and then provides appropriate control limits for a control chart. Only the usual conditions for a control chart setting, i.e., Phase I in-control pre-samples are available and subgroup observations are independent and identically distributed, are assumed.

In this article, a Shewhart-type chart and two PBCs, named maximum likelihood estimation bootstrap (MLE-b) chart and moment estimation bootstrap (MME-b) chart, for monitoring BTX percentiles are studied. The rest of this article is organized as follows: a brief introduction to the estimation methods of maximum likelihood and moment for BTX distribution parameters and percentiles are addressed in Section 2. Algorithms for building the Shewhart-type chart, the MLE-b chart, and the MME-b chart for BTX percentiles are provided in Section 3. Intensive Monte Carlo simulations are conducted in Section 4 to evaluate the implementations of Shewhart-type, MLE-b and MME-b charts for monitoring

BTX percentiles. An example is presented in Section 5 for illustration. Some conclusions are made in Section 6.

2. The Burr Type-X Distribution

Let $\Theta^T = (\alpha, \lambda)$; the BTX distribution of Eq. (1) has probability density function (PDF) and percentile function, respectively, defined as:

$$f(t;\Theta) = \alpha\lambda^2 2te^{-\lambda^2 t^2}\left(1 - e^{-(\lambda t)^2}\right)^{\alpha-1}, \quad t > 0, \tag{2}$$

and

$$Q_p(\Theta) = \lambda^{-1}\sqrt{-ln(1.0 - p^{1/\alpha})}, \quad 0 < p < 1. \tag{3}$$

Let $\mathcal{T} = \{t_1, t_2, \ldots, t_n\}$ denote a size n random sample drawn from the BTX distribution with PDF defined by Eq. (2). Then the log-likelihood function can be presented as

$$L(\Theta) = nln(\alpha) + 2nln(\lambda) + \sum_{i=1}^{n} ln(2t_i) - \sum_{i=1}^{n}\lambda^2 t_i^2 + (\alpha - 1)\sum_{i=1}^{n} ln\left(1 - e^{-\lambda^2 t_i^2}\right). \tag{4}$$

The maximum likelihood estimate (MLE), $\hat{\Theta}_n^T = (\hat{\alpha}_n, \hat{\lambda}_n)$, of Θ can be obtained by solving the following two nonlinear equations simultaneously,

$$\hat{\alpha}_n = \frac{n}{\sum_{i=1}^{n} -ln\left(1.0 - e^{\hat{\lambda}_n^2 t_i^2}\right)}, \tag{5}$$

$$\hat{\lambda}_n \sum_{i=1}^{n} t_i^2 = \hat{\lambda}_n(\hat{\alpha}_n - 1)\left(\sum_{i=1}^{n} \frac{t_i^2 e^{-\hat{\lambda}_n^2 t_i^2}}{1 - e^{-\hat{\lambda}_n^2 t_i^2}}\right) + \frac{n}{\hat{\lambda}_n}. \tag{6}$$

Based on $\hat{\Theta}_n$, the MLE of the 100pth percentile is given as:

$$\hat{Q}_{p,n}(\hat{\Theta}_n) = \hat{\lambda}_n^{-1}\sqrt{-ln(1.0 - p^{1/\hat{\alpha}_n})}; \quad 0 < p < 1. \tag{7}$$

The exact sampling distributions of $\hat{\alpha}_n$ and $\hat{\lambda}_n$ are not available, neither is the exact sampling distribution of $\hat{Q}_{p,n}(\hat{\Theta}_n)$. Surles and Padgett (2001) showed that the BTX distribution satisfied the regularity conditions required for the asymptotic normality of the MLE, $\hat{\Theta}_n$. Hence, it can be shown that $\sqrt{n}(\hat{\Theta}_n - \Theta) \to N(\mathbf{0}, \mathbf{I}^{-1}(\Theta))$, where $\mathbf{0}$ is a two-dimensional column vector of zeros and $\mathbf{I}(\Theta)$ is the Fisher information matrix defined by:

$$\mathbf{I}(\Theta) = \frac{-1}{n}\begin{bmatrix} E\left(\frac{\partial^2 L(\Theta)}{\partial\alpha^2}\right) & E\left(\frac{\partial^2 L(\Theta)}{\partial\alpha\partial\lambda}\right) \\ E\left(\frac{\partial^2 L(\Theta)}{\partial\lambda\partial\alpha}\right) & E\left(\frac{\partial^2 L(\Theta)}{\partial\lambda^2}\right) \end{bmatrix} = -\begin{bmatrix} I_{11} & I_{12} \\ I_{21} & I_{22} \end{bmatrix}. \tag{8}$$

Surles and Padgett (2001) gave an infinite series presentation for each entry of $\mathbf{I}(\Theta)$, and Kundu and Raqab (2005) studied the BTX distribution and provided other two different representations for each entry of $\mathbf{I}(\Theta)$. When $\alpha - 3$ is a non-negative integer, following the same derivation process as the one used by Surles and Padget (2001), each entry of $\mathbf{I}(\Theta)$ can be expressed as a finite term summation. Here, the results from Kundu and Raqab

(2005) are presented as follows: If $\alpha > 2$,

$$I_{11} = -\frac{1}{\alpha^2},$$

$$I_{12} = I_{21} = \frac{2}{\lambda^2(\alpha-1)}\left((\varphi(\alpha) - \varphi(1)) - \frac{\alpha-1}{\alpha}\right),$$

$$I_{22} = -\frac{2}{\lambda^2}[1 + \varphi(\alpha+1) - \varphi(1)] - \frac{2\alpha}{\lambda^3}[\varphi(1) - \varphi(\alpha)] - \frac{2(\alpha-1)}{\lambda^3} - \frac{4\alpha}{\lambda^3(\alpha-2)}[(\varphi(2) - \varphi(\alpha))^2 + \varphi'(2) - \varphi'(\alpha)],$$

and if $0 < \alpha \leq 2$,

$$I_{11} = -\frac{1}{\alpha^2},$$

$$I_{12} = I_{21} = \frac{2\alpha}{\lambda^2}\left(\int_0^\infty x e^{-2x}(1-e^{-x})^{\alpha-2}dx\right),$$

$$I_{22} = -\frac{2}{\lambda^2}[1 + \varphi(\alpha+1) - \varphi(1) - \frac{\alpha(\alpha-1)}{\lambda}\int_0^\infty x e^{-2x}(1-2x-e^{-x})(1-e^{-x})^{\alpha-3}dx],$$

where $\varphi(t)$ is the digamma function and $\varphi'(t)$ is the derivative of $\varphi(t)$. It can be shown that

$$\frac{\hat{Q}_{p,n}(\hat{\Theta}_n) - Q(p;\Theta)}{\sigma^2_{p,n}} \to N(0,1),$$

where

$$\sigma^2_{p,n} = \frac{1}{n}\nabla Q(\Theta)^T \mathbf{I}^{-1}(\Theta)\nabla Q(\Theta),$$

and $\nabla Q(\Theta)$ is the gradient of $Q(\Theta)$ with respect to Θ. Therefore, the Shewhart-type chart can be constructed, based on asymptotical normal distribution, to monitor the BTX percentile. Because the evaluations of Fisher information matrix formulas, provided by Surles and Padgett (2001) and Kundu and Raqab (2005), respectively, need complicate computation skills, both Fisher information matrix formulas are difficult to be used practically. Therefore, the observed Fisher information matrix without taking expectation, presented as follows, is used instead of $\mathbf{I}(\Theta)$:

$$\hat{\mathbf{I}}_{\mathbf{n}}(\hat{\Theta}_n) = \frac{-1}{n}\left[\begin{array}{cc} \frac{\partial^2 L(\Theta)}{\partial\alpha^2} & \frac{\partial^2 L(\Theta)}{\partial\alpha\partial\lambda} \\ \frac{\partial^2 L(\Theta)}{\partial\lambda\partial\alpha} & \frac{\partial^2 L(\Theta)}{\partial\lambda^2} \end{array}\right]_{\Theta=\hat{\Theta}_n}. \tag{9}$$

Denote ARL_0 and ARL_1 as in-control and out-of-control ARLs, respectively. According to simulation results, reported in Section 4, it could be found that the simulated ARL_0 of the Shewhart-type chart seriously underestimates the corresponding nominal ARL_0. Hence, the Shewhart-type chart based on the MLE, $\hat{Q}_{p,n}$, will not be recommended to monitor BTX percentiles in practice.

Let T be the BTX distribution random variable. The following moments for the BTX distribution have been provided by Kundu and Raqab (2005) and also can be found in Lio et al. (2011):

$$E(T^2) = (\varphi(\alpha+1) - \varphi(1))/\lambda^2, \tag{10}$$

$$E[T^4] - [E[T^2]]^2 = (-\varphi'(\alpha+1) + \varphi'(1))/\lambda^4. \tag{11}$$

Equating sample moments to the corresponding population moments, the following equations can be used to find the moment method estimate (MME), $\tilde{\Theta}_n^T = (\tilde{\alpha}_n, \tilde{\lambda}_n)$, of $\Theta^T = (\alpha, \lambda)$:

$$\varphi(\tilde{\alpha}_n+1) - \varphi(1) = \frac{\tilde{\lambda}_n^2}{n}\left[\sum_i^n t_i^2\right], \tag{12}$$

$$-\varphi'(\tilde{\alpha}_n+1) + \varphi'(1) = \frac{\tilde{\lambda}_n^4}{n}\left[\sum_i^n t_i^4\right] - \frac{\tilde{\lambda}_n^4}{n^2}\left[\sum_i^n t_i^2\right]^2. \tag{13}$$

After a simple algebra process, the solution for $\tilde{\alpha}_n$ can be obtained via the following equation:

$$\frac{[\varphi(\tilde{\alpha}_n+1) - \varphi(1)]^2}{[\varphi(\tilde{\alpha}_n+1) - \varphi(1)]^2 + \varphi'(1) - \varphi'(\tilde{\alpha}_n+1)} = \frac{\left[\sum_i^n t_i^2\right]^2}{n\left[\sum_i^n t_i^4\right]} \tag{14}$$

and the solution of $\tilde{\lambda}_n$ can be obtained via the following equation:

$$\tilde{\lambda}_n = \left[\frac{n\varphi(\tilde{\alpha}_n+1) - \varphi(1)}{\sum_i^n t_i^2}\right]^{1/2}. \tag{15}$$

Then, the BTX percentile $Q_p(\Theta)$ based on MME, $\tilde{\Theta}_n$, can be computed and denoted by $\tilde{Q}_{p,n}(\tilde{\Theta}_n)$. However, the exact sampling distributions of $\tilde{\Theta}_n$ and $\tilde{Q}_{p,n}(\tilde{\Theta}_n)$ are not available.

3. The Shewhart-Type and Parametric Bootstrap Charts

In Phase I, it is assumed that k in-control pre-samples of each size m are drawn from the BTX distribution of Eq. (1) for the control chart setting. Let $n = m \times k$ denote the total sample size used in Phase I. A Shewhart-type chart and two PBCs are constructed in the following subsections.

3.1. *Shewhart-Type Chart*

According to the estimation procedure described in Section 2, the MLE of the 100pth percentile based on each size m pre-sample from a Phase I in-control process can be obtained via $\hat{Q}_{p,m}(\hat{\Theta}_m) = \hat{\lambda}_m^{-1}\sqrt{-ln(1.0 - p^{1/\hat{\alpha}_m})}$, where $\hat{\Theta}_m$ is the MLE of Θ. Then, the Shewhart-type chart for monitoring the 100pth percentile, $Q_p(\Theta)$, can be constructed as follows:

1. Using n sample observations from Phase I in-control process, the MLE, $\hat{\Theta}_n^T = (\hat{\alpha}_n, \hat{\lambda}_n)$, via Eqs. (5) and (6), is obtained and the asymptotic standard error of

$\hat{Q}_{p,m}(\hat{\Theta}_m)$ can be estimated by

$$\mathrm{SE}_{Q_m} = \sqrt{\frac{1}{m}\nabla Q_p^T(\hat{\Theta}_n)\hat{\mathbf{I}}_n(\hat{\Theta}_n)\nabla Q_p(\hat{\Theta}_n)}.$$

2. For the jth pre-sample of size m, the MLE of $Q_p(\Theta)$ is obtained using Eqs. (5)–(7) and denoted by $\hat{Q}^j_{p,m}(\hat{\Theta}^j_m)$, $j = 1, 2, \ldots, k$. The sample mean of $\hat{Q}^j_{p,m}(\hat{\Theta}^j_m)$, $j = 1, 2, \ldots, k$, is computed and labeled as

$$\bar{\hat{Q}}_{p,m}(\hat{\Theta}_m) = \frac{1}{k}\sum_{j=1}^{k}\hat{Q}^j_{p,m}\left(\hat{\Theta}^j_m\right).$$

3. The control limits of the Shewhart-type chart are presented as follows:

$$\mathrm{UCL_{SH}} = \bar{\hat{Q}}_{p,m}(\hat{\Theta}_m) + z_{(1-\gamma/2)} \times \mathrm{SE}_{Q_m},$$
$$\mathrm{LCL_{SH}} = \bar{\hat{Q}}_{p,m}(\hat{\Theta}_m) - z_{(1-\gamma/2)} \times \mathrm{SE}_{Q_m},$$

and the center line (CL) is $\mathrm{CL_{SH}} = \bar{\hat{Q}}_{p,m}(\hat{\Theta}_m)$, where $\Phi(z_\delta) = \delta$, $0 < \delta < 1$, $\Phi(.)$ is the standard normal CDF, and γ is a given false alarm rate (FAR).

After the control limits of the Shewhart-type chart are determined based on Phase I in-control samples, future samples of each size m (Phase II samples) are drawn from the BTX process to compute the plot statistic $\hat{Q}_{p,m}(\hat{\Theta}_m)$. If $\hat{Q}_{p,m}(\hat{\Theta}_m)$ is plotted between control limits, $\mathrm{LCL_{SH}}$ and $\mathrm{UCL_{SH}}$, then the process is assumed to be in control. Otherwise, signal the process out-of-control.

3.2. *Bootstrap Charts*

The PBC based on MLE for monitoring BTX percentiles is constructed according to the following steps:

1. Use n sample observations from Phase I in-control process, to obtain the MLE, $\hat{\Theta}^T_n = (\hat{\alpha}_n, \hat{\lambda}_n)$, via Eqs. (5) and (6).
2. Generate m parametric bootstrap observations from the BTX distribution of Eq. (1) but replacing α and λ by the corresponding MLEs, $\hat{\alpha}_n$ and $\hat{\lambda}_n$, obtained from Step 1. Denote these parametric bootstrap observations by $x^*_1, x^*_2 \ldots, x^*_m$.
3. Find the MLEs of α and λ using parametric bootstrap observations, $x^*_1, x^*_2 \ldots, x^*_m$, and denote the obtained MLEs by $\hat{\alpha}^*_m$ and $\hat{\lambda}^*_m$, respectively.
4. Compute the bootstrap estimate of the $100p$th percentile according to the formula:

$$\hat{q}^*_p = \hat{Q}^*_{p,m}(\hat{\Theta}) = \sqrt{-ln\left(1.0 - p^{1/\hat{\alpha}^*_m}\right)}/\hat{\lambda}^*_m.$$

5. Repeat Steps 2–4 B times to obtain a size B bootstrap sample, $\hat{q}^*_{p,1}, \hat{q}^*_{p,2}, \ldots, \hat{q}^*_{p,B}$, where B is a given large positive integer.
6. Given a FAR γ, find the $(\gamma/2)$th and $(1-\gamma/2)$th empirical quantiles of the bootstrap sample, $\hat{q}^*_{p,1}, \hat{q}^*_{p,2}, \ldots, \hat{q}^*_{p,B}$ as the lower control limit (LCL) and upper control limit (UCL), respectively. The method to find sample quantiles, proposed by Hyndman and Fan (1996), will be used for the simulation study in Section 4.

The above bootstrap chart is called MLE-b chart. Similarly, if the MLEs, $\hat{\alpha}(\hat{\alpha}^*)$ and $\hat{\lambda}(\hat{\lambda}^*)$, of α and λ are replaced by the MMEs, $\tilde{\alpha}(\tilde{\alpha}^*)$ and $\tilde{\lambda}(\tilde{\lambda}^*)$, respectively, and MLE method is replaced by MME method from Step 1 to Step 3, then the corresponding bootstrap chart is constructed based on moment method, and is called MME-b chart. The plot statistic for MLE-b chart is $\hat{Q}_{p,m}(\hat{\Theta}_m)$ and the plot statistic for MME-b chart is $\tilde{Q}_{p,m}(\tilde{\Theta}_m)$.

4. Simulation Study

To examine the performance of these three BTX percentile control charts, discussed in Section 3, an intensive Monte Carlo simulation study was conducted using R language (R Development Core Team, 2006) that was originally developed by Ihaka and Gentleman (1996). The R source codes can be obtained from authors upon request.

The performance of BTX percentile control charts are investigated in terms of simulated ARL_0 and ARL_1 and the standard errors of run lengths (SERLs), respectively. Moreover, the average of UCLs and LCLs and their associated standard errors are also evaluated through simulation. Simulation has been carried out with different sample sizes, different percentiles of interest, and different levels of FARs. Ten thousand bootstrap repetitions, $B = 10,000$, have been used to determine the control limits for each bootstrap chart. Moreover, all complete procedures, introduced in Section 3, have been repeated 10,000 times to evaluate the ARL values, the associated SERL values, and the standard errors of control limits. For brevity, some simulation results are displayed in Tables 1–9. It should be mentioned that when subgroup size is small such as $m = 4$, 5, or 6, the iterative procedure for solving the

Table 1
Simulated ARL_0 and SERL values from the Shewhart-type chart for $p = 0.1$, $k = 20$, and $\lambda = 1$

Nominal ARL_0	α	$m = 4$		$m = 5$		$m = 6$	
		ARL_0	SERL	ARL_0	SERL	ARL_0	SERL
10	0.5	6.105	0.063	6.587	0.067	7.257	0.073
	1.0	7.977	0.077	8.226	0.079	8.500	0.081
	2.0	8.649	0.086	8.865	0.088	8.928	0.089
	5.0	8.888	0.089	8.772	0.088	8.758	0.086
100	0.5	17.665	0.228	18.792	0.237	21.448	0.277
	1.0	54.147	0.723	57.071	0.729	60.110	0.754
	2.0	82.353	1.008	82.866	1.027	82.226	0.962
	5.0	83.101	1.209	80.882	1.005	81.336	1.001
370	0.5	25.979	0.429	27.297	0.363	32.634	0.462
	1.0	114.741	1.741	127.015	1.885	135.596	1.922
	2.0	264.998	3.802	265.860	3.641	266.605	3.521
	5.0	295.222	4.724	279.897	4.148	286.145	3.872
500	0.5	28.446	0.509	29.624	0.400	35.924	0.511
	1.0	136.543	2.080	152.967	2.289	161.178	2.319
	2.0	338.687	4.956	339.096	5.082	346.583	4.884
	5.0	391.220	6.352	369.691	5.451	378.485	5.464

Table 2
Simulated ARL_0 and SERL values from the MLE-b chart for $p = 0.1$, $k = 20$, and $\lambda = 1$

		$m = 4$		$m = 5$		$m = 6$	
Nominal ARL_0	α	ARL_0	SERL	ARL_0	SERL	ARL_0	SERL
10	0.5	9.361	0.092	9.38	0.092	9.32	0.091
	1.0	9.453	0.094	9.32	0.093	9.31	0.094
	2.0	9.413	0.095	9.57	0.097	9.31	0.092
100	0.5	92.329	1.126	92.365	1.091	90.913	1.016
	1.0	97.578	1.257	93.864	1.143	91.292	1.078
	2.0	97.815	1.367	97.043	1.233	94.976	1.216
370	0.5	354.592	5.177	352.867	4.882	336.705	4.407
	1.0	366.589	5.707	365.999	5.538	355.775	4.964
	2.0	396.656	6.808	383.682	5.860	361.026	5.217
500	0.5	485.613	7.233	485.095	6.779	453.055	6.040
	1.0	509.068	8.262	510.362	8.141	477.215	6.718
	2.0	542.770	9.574	519.847	8.065	498.641	7.457

MMEs of BTX parameters is often divergent. Hence, only some simulation results with subgroup size, $m = 10$, for the MME-b chart are given in Tables 3, 7 and 8.

Table 1 shows that the simulated ARL_0 for the Shewhart-type chart seriously underestimates the nominal ARL_0 due to producing a narrow band of control limits. This means that the Shewhart-type chart will incur a higher FAR than expectation. Tables 2 and 3

Table 3
Simulated ARL_0 and SERL values from the MME-b chart for $p = 0.10$, $m = 10$, $k = 20$, and $\lambda = 1$

		$m = 4$		$m = 5$		$m = 6$	
Nominal ARL_0	α	ARL	SERL	ARL	SERL	ARL	SERL
10	0.5	9.050	0.0872	9.079	0.0909	9.2659	0.09458
	1.0	9.074	0.0881	9.109	0.0903	9.425	0.0971
	10.0	9.423	0.0980	9.431	0.0982	9.422	0.0961
100	0.5	84.857	0.9567	87.743	1.0411	94.0007	1.33539
	1.0	88.830	1.0018	93.182	1.1219	96.6795	1.3739
	10.0	91.192	1.0731	95.358	1.2645	96.196	1.3069
370	0.5	314.030	3.9772	332.903	4.5686	372.3344	6.8524
	1.0	329.580	4.0352	342.444	4.6120	396.4732	7.7491
	10.0	361.294	4.7038	361.989	5.3724	389.464	6.8079
500	0.5	427.093	5.7029	450.158	6.4289	505.2284	9.95987
	1.0	445.364	5.7365	467.153	6.4625	544.0697	7.74910
	10.0	484.452	6.3274	502.739	7.9250	544.070	10.1513

Table 4
Simulated ARL_0 and SERL values from the MLE-b chart for $(\alpha, \lambda) = (10, 1)$ and $k = 20$

		$p = 0.10$		$p = 0.25$		$p = 0.50$	
Nominal ARL_0	m	ARL_0	SERL	ARL_0	SERL	ARL_0	SERL
10	4	9.6474	0.101	9.463	0.100	9.258	0.093
	6	9.3354	0.093	9.373	0.094	9.425	0.093
	10	9.2757	0.093	9.525	0.093	9.180	0.089
100	4	102.983	1.532	100.517	1.507	97.489	1.354
	6	95.890	1.280	95.672	1.238	93.979	1.156
	10	93.220	1.125	93.478	1.113	89.046	1.019
370	4	408.713	7.235	386.656	6.585	366.975	5.781
	6	376.712	5.790	363.965	5.682	362.571	5.464
	10	353.738	4.843	350.907	4.928	333.125	4.442
500	4	543.428	9.193	509.780	8.387	495.615	7.981
	6	500.991	7.740	490.212	7.798	484.795	7.344
	10	481.410	6.639	473.318	6.730	455.741	6.470

show that the simulated ARL_0s for MLE-b and MME-b charts are close to their corresponding nominal ARL_0s. In general, MLE-b and MME-b charts outperform the Shewhart-type chart in terms of the simulated ARL_0. Table 4 gives the simulated ARL_0 and the associated SERL when the MLE-b chart is used with various subgroup sizes for numerous percentiles. It could be found that the MLE-b chart performs satisfactorily in terms of the simulated

Table 5
Simulated average estimates of LCL and UCL from the MLE-b chart for $(\alpha, \lambda) = (10, 1)$ and $k = 20$

		$p = 0.10$		$p = 0.25$		$p = 0.50$	
Nominal ARL_0	m	LCL	UCL	LCL	UCL	LCL	UCL
10	4	1.042	1.662	1.218	1.763	1.382	1.937
	6	1.068	1.573	1.248	1.691	1.427	1.882
	10	1.100	1.490	1.282	1.624	1.473	1.826
100	4	0.886	1.862	1.089	1.952	1.253	2.128
	6	0.939	1.732	1.139	1.837	1.317	2.032
	10	0.998	1.610	1.196	1.733	1.385	1.938
370	4	0.820	1.966	1.034	2.051	1.198	2.228
	6	0.883	1.811	1.093	1.911	1.270	2.107
	10	0.954	1.667	1.158	1.786	1.347	1.992
500	4	0.804	3.264	1.021	3.052	1.184	3.524
	6	0.869	1.825	1.082	1.925	1.258	2.122
	10	0.943	1.678	1.149	1.795	1.337	2.002

Table 6
The standard errors of the control limits in Table 5

		$p = 0.10$		$p = 0.25$		$p = 0.50$	
Nominal ARL_0	m	SE_{LCL}	SE_{UCL}	SE_{LCL}	SE_{UCL}	SE_{LCL}	SE_{UCL}
10	4	0.0005	0.0003	0.0004	0.0004	0.0003	0.0005
	6	0.0004	0.0002	0.0003	0.0003	0.0002	0.0003
	10	0.0003	0.0002	0.0002	0.0002	0.0002	0.0002
100	4	0.0006	0.0004	0.0005	0.0005	0.0004	0.0006
	6	0.0004	0.0003	0.0003	0.0003	0.0003	0.0004
	10	0.0003	0.0002	0.0002	0.0002	0.0002	0.0003
370	4	0.0006	0.0006	0.0005	0.0006	0.0004	0.0007
	6	0.0005	0.0004	0.0004	0.0004	0.0003	0.0005
	10	0.0003	0.0002	0.0003	0.0002	0.0002	0.0003
500	4	0.0006	0.4821	0.0005	0.4382	0.0004	0.5206
	6	0.0005	0.0004	0.0004	0.0004	0.0003	0.0005
	10	0.0003	0.0002	0.0003	0.0003	0.0002	0.0003

ARL_0. Tables 5 and 6 show the average values of simulated LCLs and UCLs and their associated standard errors when the MLE-b chart is used. Tables 7 and 8 exhibit the average values of simulated LCLs and UCLs and their associated standard errors for the MME-b chart. Again, it can be seen that the standard errors of the LCL and UCL are usually smaller for both MLE-b and MME-b charts. That is, the proposed constructing procedures for

Table 7
Simulated average estimates of LCL and UCL from the MME-b chart for $p = 0.10, 0.25, 0.50$, $m = 10$, $k = 20$, and $\lambda = 1$

		$p = 0.10$		$p = 0.25$		$p = 0.50$	
Nominal ARL_0	α	LCL	UCL	LCL	UCL	LCL	UCL
10	0.5	0.031	0.421	0.120	0.595	0.330	0.855
	1.0	0.163	0.680	0.346	0.853	0.608	1.106
	10.0	1.086	1.514	1.280	1.638	1.476	1.829
100	0.5	0.004	0.576	0.040	0.752	0.205	1.022
	1.0	0.057	0.838	0.196	1.004	0.476	1.259
	10.0	0.921	1.633	1.173	1.748	1.387	1.941
370	0.5	0.001	0.651	0.022	0.827	0.158	1.101
	1.0	0.031	0.914	0.138	1.075	0.414	1.331
	10.0	0.829	1.689	1.117	1.800	1.349	1.994
500	0.5	0.001	0.665	0.019	0.841	0.148	1.115
	1.0	0.026	0.927	0.125	1.088	0.399	1.344
	10.0	0.804	1.699	1.101	1.810	1.340	2.004

Table 8
The standard deviations of the control limits in Table 7

		$p = 0.10$		$p = 0.25$		$p = 0.50$	
Nominal ARL_0	α	LCL	UCL	LCL	UCL	LCL	UCL
10	0.5	0.0001	0.0003	0.0003	0.0003	0.0004	0.0004
	1.0	0.0003	0.0003	0.0004	0.0003	0.0004	0.0003
	10.0	0.0004	0.0002	0.0003	0.0002	0.0002	0.0002
100	0.5	0.0000*	0.0003	0.0001	0.00040	0.0004	0.0005
	1.0	0.0002	0.0003	0.0004	0.00037	0.0004	0.0004
	10.0	0.0005	0.0002	0.0004	0.00027	0.0002	0.0003
370	0.5	0.0000	0.0004	0.0001	0.0004	0.0003	0.0005
	1.0	0.0001	0.0003	0.0003	0.0004	0.0005	0.0005
	10.0	0.0006	0.0002	0.0004	0.0003	0.0002	0.0003
500	0.5	0.0000*	0.0004	0.0000*	0.0004	0.0003	0.0005
	1.0	0.0001	0.0003	0.0003	0.0004	0.0005	0.0005
	10.0	0.0006	0.0002	0.0004	0.0003	0.0003	0.0003

*Indicates the value < 0.0001.

MLE-b and MME-b charts can provide stable control limits and are helpful to construct a MLE-b or MME-b chart in practical applications. Hence, the Shewhart-type chart will not be recommended and only two proposed PBCs will be examined in the following study.

Table 9
Simulated ARL_1 and SERL values when α shifts to α_1 from α_0 for $m = 10$, $k = 20$, and $\lambda = 1$

γ	p	α_0	α_1	ARL_1(MLE)	SERL	ARL_1(MME)	SERL
0.1	0.10	1.0	0.5	1.4395	0.008	2.424	0.021
		10.0	5.0	1.4597	0.008	1.783	0.013
		10.0	8.0	5.3278	0.056	6.635	0.072
	0.25	2.0	0.5	1.0091	0.001	1.032	0.001
0.01	0.10	1.0	0.5	2.4548	0.020	10.078	0.130
		10.0	5.0	2.6212	0.023	6.797	0.091
		10.0	8.0	31.2233	0.430	61.988	0.896
	0.25	2.0	0.5	1.0368	0.002	1.233	0.005
0.0027	0.10	1.0	0.5	3.541	0.034	23.667	0.367
		10.0	5.0	3.973	0.042	20.465	0.350
		10.0	8.0	92.378	1.696	233.799	3.762
	0.25	2.0	0.5	1.065	0.002	1.603	0.012
0.002	0.10	1.0	0.5	3.897	0.039	29.390	0.462
		10.0	5.0	4.439	0.048	28.030	0.536
		10.0	8.0	120.113	2.302	330.704	5.577
	0.25	2.0	0.5	1.074	0.002	1.759	0.014

The main concern is the downward shift of distribution percentile, which indicates a deteriorating quality in the product lifetime. First, control limits of the MLE-b and MME-b charts are established based on generated in-control Phase I subgroups; then further subgroups are generated from an out-of-control process and used for evaluating the ARL_1 and its standard errors. It could be shown that the BTX percentile decreases with respect to α when λ is given. Hence, to implement an out-of-control process from an in-control process, we may decrease the value of shape parameter, α, from α_0 value for an in-control process to a smaller value, α_1, for an out-of-control process. For brevity, part of out-of-control cases and the corresponding ARL_1 values for MLE-b and MME-b charts are displayed in Table 9. In view of Table 9, the ARL_1 values and the associated SERLs are very small. Therefore, these simulation results support that both MLE-b and MME-b charts are capable of monitoring out-of-control BTX percentiles.

5. Illustrative Examples

Bader and Priest (1982) obtained strength data (measured in GPa) for single carbon fibers and impregnated 1,000 carbon fiber tows. Single fibers were tested under tension at gauge lengths of 1, 10, 20, and 50 millimeter (mm). Impregnated tows of 1,000 fibers were tested at gauge lengths of 20, 50, 150, and 300 mm. Durham and Padgett (1997) demonstrated that the Weibull model did not provide a goodness of fit to these datasets. Surles and Padgett (1998, 2001) suggested that the BTX distribution could be used with pleasing results to model these datasets. Surles and Padgett (1998, 2001) provided maximum likelihood estimation results for the single fibers of 20 and 50 mm in gauge length under BTX model with common scale parameter or different scale parameter model setting. In their studies, the MLEs of shape parameters in the 20 mm single fiber modeling and the 50 mm single fiber modeling were around 10 and the MLEs of scale parameters under different scale parameter setting were very close to 1. Surles and Padgett (2001) also conducted an intensive simulation study based on what they called typical case with $\alpha = 10$.

In this section, the MLE-b and MME-b charts are applied to monitoring the strength of single fiber of 20 mm in gauge. Since the datasets provided by Bader and Priest (1982) were not for the purpose of constructing control charts originally, hence the reported datasets by Bader and Priest (1982) cannot be used directly. In this example, 20 subgroups of each 10 fiber strengths are simulated independently from an in-control BTX process with $\alpha_0 = 10$ and $\lambda = 1$ of which 10th percentile is found as $Q(0.10, \alpha, \lambda) = 1.258$. These 20 in-control

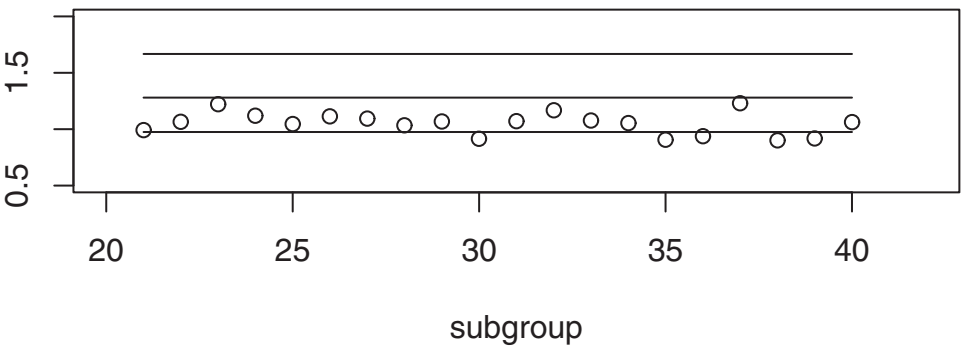

Figure 1. The MLE-b chart for the strength data of single fiber with FAR = 0.0027.

Table 10
Top 20 subgroups of strength of single fiber of 20 mm in gague length generated from the BTX distribution with $\alpha_0 = 10$ and $\lambda = 1$

Subgroup number	Strength observations									
1	1.558	1.043	2.131	1.555	2.004	1.237	1.038	1.367	1.116	1.480
2	1.741	1.634	2.450	1.948	1.585	1.559	1.658	2.006	1.100	2.009
3	1.573	1.624	2.236	2.010	1.856	2.840	1.677	1.993	1.334	1.663
4	1.599	2.518	1.693	1.772	1.930	1.367	1.675	0.958	1.283	1.716
5	1.799	2.525	1.847	1.711	1.748	1.619	1.490	2.956	1.334	1.832
6	1.581	1.629	1.370	1.379	1.337	1.751	1.537	1.822	1.367	1.550
7	1.439	1.887	1.378	1.785	1.553	1.289	2.158	2.084	1.381	1.406
8	2.268	1.793	1.282	2.395	1.749	1.464	1.281	1.456	1.293	1.795
9	2.015	1.663	1.872	1.911	1.670	1.496	1.820	1.783	1.656	1.346
10	1.681	1.798	1.781	1.411	1.798	1.236	1.024	1.520	1.823	1.531
11	2.282	1.714	2.368	1.128	1.693	1.433	1.229	1.561	1.536	1.907
12	1.369	1.721	1.888	1.763	1.567	1.607	1.528	1.745	1.087	1.575
13	1.862	1.817	1.694	1.829	1.467	1.595	1.853	1.682	1.856	2.090
14	2.116	1.839	1.494	1.816	1.722	1.641	1.014	2.139	1.524	1.376
15	1.077	1.340	2.342	2.033	2.068	1.590	1.725	2.192	1.503	1.942
16	1.937	1.385	1.667	1.384	1.542	1.354	1.383	1.531	1.519	2.140
17	1.486	1.908	1.302	2.099	1.305	1.496	1.543	1.625	1.523	1.729
18	1.323	1.978	1.713	2.060	2.304	1.396	1.980	1.791	1.262	1.465
19	2.007	2.147	1.649	1.678	2.241	1.846	1.924	2.490	1.619	2.343
20	1.328	1.445	2.330	1.450	1.698	1.323	2.096	1.598	1.458	2.561

subgroups are reported in Table 10. Assume that the process parameter α shifts to $\alpha_1 = 5$ after the first 20 in-control subgroups. Another 20 out-of-control subgroups of each 10 fiber strengths are generated from the BTX distribution with $\alpha = 5$ and $\lambda = 1$ and reported in Table 11.

The MLE-b and MME-b charts are established based on the 20 in-control subgroups of each 10 fiber strengths, reported in Table 10, with FAR = 0.0027 and $B = 10,000$. The control limits of the MLE-b chart are obtained as

$$\mathrm{UCL}_{\mathrm{MLE-b}} = 1.667,$$
$$\mathrm{LCL}_{\mathrm{MLE-b}} = 0.975,$$

and the CL of the MLE-b chart is $\mathrm{CL}_{\mathrm{SH}} = 1.279$. The control limits of the MME-b chart are obtained as

$$\mathrm{UCL}_{\mathrm{MME-b}} = 1.731,$$
$$\mathrm{LCL}_{\mathrm{MME-b}} = 0.841,$$

and the CL of the MME-b chart is $\mathrm{CL}_{\mathrm{SH}} = 1.271$. Figures 1 and 2 show that the MLE-b and MME-b charts provide asymmetric control limits from their respective CL. In the MLE-b chart, the first out-of-control signal is observed at subgroup 30, there are five points below

Table 11
Twenty out-of-control subgroups of strength of single fiber of 20 mm in gague length generated from the BTX distribution with $\alpha_1 = 5.0$ and $\lambda = 1$

Subgroup number	Strength observations									
21	1.502	1.417	0.821	1.363	1.165	1.047	1.493	1.571	2.121	1.543
22	1.862	0.898	1.051	1.968	1.662	1.903	1.335	1.502	1.665	1.344
23	2.114	1.156	1.520	1.436	1.294	1.370	2.411	1.694	1.758	1.549
24	1.431	1.932	1.365	2.001	1.992	1.144	1.185	1.359	1.390	1.151
25	1.831	2.047	1.336	1.179	1.245	1.586	1.518	1.618	0.844	1.428
26	1.839	1.488	1.250	2.246	1.721	1.634	1.500	0.945	1.837	1.196
27	1.405	1.260	1.065	1.345	1.124	1.697	1.599	1.101	1.757	1.553
28	1.133	1.924	1.028	1.873	1.543	1.570	0.887	1.395	1.326	1.625
29	2.300	1.396	1.689	1.724	0.989	0.854	1.783	1.907	1.760	2.124
30	1.372	1.475	1.045	1.266	1.357	1.681	1.295	0.671	2.161	1.528
31	1.104	2.073	1.840	1.614	0.988	1.353	1.344	1.418	1.545	2.604
32	1.604	1.680	1.125	1.717	1.796	1.603	1.318	1.278	1.106	1.788
33	1.579	1.230	1.343	1.301	2.259	1.086	2.136	1.069	1.614	1.545
34	1.433	3.066	1.351	1.836	1.068	1.310	1.250	1.246	1.495	1.652
35	1.290	0.774	1.635	1.107	1.138	1.257	1.379	0.902	1.321	1.497
36	2.166	1.268	2.003	0.980	0.755	1.550	1.645	1.174	2.395	1.986
37	1.653	1.889	1.536	2.186	2.129	1.418	0.935	1.602	1.998	1.929
38	1.651	1.627	1.242	1.772	1.555	1.038	2.185	0.972	0.756	1.280
39	1.199	1.327	1.322	1.430	1.436	1.054	1.149	1.261	2.833	0.905
40	1.325	0.994	1.006	2.260	1.306	1.786	1.612	1.396	1.855	1.625

the LCL, and no point above the UCL. In the MME-b chart, the first out-of-control signal is observed at subgroup 34, there are two points below the LCL, and one case above the CL. Therefore, it can be seen that the MLE-b chart seems to signal out-of-control earlier than the MME-b chart when the process is out-of-control.

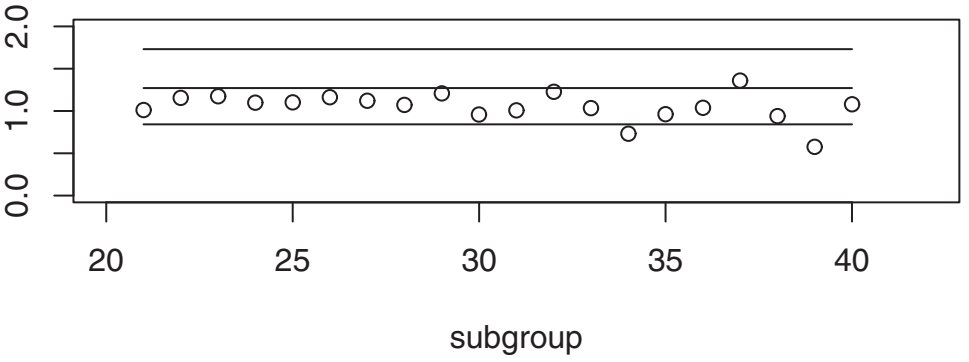

Figure 2. The MME-b chart for the strength data of single fiber with FAR = 0.0027.

6. Conclusions

A Shewhart-type chart and two PBCs have been constructed for monitoring BTX percentiles. The Shewhart-type control chart is constructed based on the asymptotic normal distribution of maximum likelihood estimator and delta method. Because the Shewhart-type chart cannot provide adequate control limits, PBCs based on MLE and MME, respectively, are proposed for monitoring BTX percentiles. Through an intensive Monte Carlo simulation, it has been found that when subgroup size is small (such as 3, 4, 5, or 6) the MLE-b chart is much easier to be constructed than the MME-b chart because the MMEs of BTX parameters are difficult to be obtained. When subgroup size grows to 10 or larger, the proposed PBCs could be established accurately for monitoring BTX percentiles and could signal out-of-control quickly when the process shifts to out-of-control. Generally, the MLE-b chart is more efficient than the MME-b chart to alarm for process out-of-control. Therefore, the MLE-b chart would be recommended for monitoring BTX percentiles practically.

Extending the developed procedures of control charts in Section 3 for monitoring the percentiles of other important life distributions is of great interest and will be investigated in the future.

Acknowledgments

The authors thank the editor, associate editor, and anonymous referee for their comments and suggestions, which significantly improved this article.

References

Ahmad, K. E., Fakhry, M. E., Jaheen, Z. F. (1997). Empirical Bayes estimation of $P(Y < X)$ and characterization of Burr-type X model. *Journal of Statistical Planning and Inference* 64:297–308.

Bader, M. G., Priest, A. M. (1982). Statistical aspects of fiber and bundle strength in hybrid composites. In: Hayashi, T., Kawata, K., Umekawa, S., eds. *Progress in Science and Engineering Composites*. Tokyo: ICCM-IV, pp. 1129–1136.

Bajgier, S. M. (1992). The use of bootstrapping to construct limits on control charts. In: *Proceedings of the Decision Science Institute, San Diego, CA*, pp. 1611–1613.

Burr, I. W. (1942). Cumulative frequency functions. *Annals of Mathematical Statistics* 13:215–222.

Durham, S. D., Padgett, W. J. (1997). Cumulative damage models for system strength with application to carbon fibers and composites. *Technometrics* 39:34–44.

Efron, B., Tibshirani, R. J. (1993). *An Introduction to the Bootstrap*. New York: Chapman & Hall.

Gunter, B. (1992). Bootstrapping: How to make something from almost nothing and get statistically valid answers, Part III. *Quality Progress* 25:119–122.

Hyndman, R. J., Fan, Y. (1996). Sample quantiles in statistical packages. *American Statistician* 50:361–365.

Ihaka, R., Gentleman, R. (1996). R: A language for data analysis and graphics. *Journal of Computational and Graphical Statistics* 5:299–314.

Jaheen, Z. F. (1995). Bayesian approach to prediction with outliers from the Burr type X model. *Microelectronics Reliability* 35:45–47.

Jaheen, Z. F. (1996). Empirical Bayes estimation for the reliability and failure rate functions of the Burr type X failure model. *Journal of Applied Statistical Science* 3:281–288.

Jones, L. A., Woodall, W. Y. (1998). The performance of bootstrap control charts. *Journal of Quality Technology* 30:362–375.

Kundu, D., Raqab, M. Z. (2005). Generalized Rayleigh distribution: Different method of estimations. *Computational Statistics & Data Analysis* 49:187–200.

Lio, Y. L., Chen, D.-G., Tsai, T.-R. (2011). Parameter estimations for generalized Rayleigh distribution under progressively type I interval censored data. *American Open Journal of Statistics* 1:46–57.

Lio, Y. L., Park, C. (2008). A bootstrap control chart for Birnbaum-Saunders percentiles. *Quality and Reliability Engineering International* 24:585–600.

Lio, Y. L., Park, C. (2010). A bootstrap control chart for inverse Gaussian percentiles. *Journal of Statistical Computation and Simulation* 80:287–299.

Liu, R. Y., Tang, J. (1996). Control charts for dependent and independent measurements based on the bootstrap. *Journal of the American Statistical Association* 91:1694–1700.

Mudholkar, G. S., Srivastava, D. K. (1993). Exponentiated Weibull family for analyzing bathtub failure-rate data. *IEEE Transactions on Reliability* 42:299–302.

Mudholkar, G. S., Srivastava, D. K. (1995). The exponentiated Weibull family: A reanalysis of the bus-motor-failure data. *Technometrics* 37:436–445.

Nichols, M. D., Padgett, W. J. (2005). A bootstrap control chart for Weibull percentiles. *Quality and Reliability Engineering International* 22:141–151.

Onar, A., Padgett, W. J. (2000). Accelerated test models with the inverse Gaussian distributions. *Journal of Statistical Planning and Inference* 89:119–133.

Padgett, W. J., Spurrier, J. D. (1990). Shewhart-type charts for percentiles of strength distributions. *Journal of Quality Technology* 22:283–288.

R Development Core Team. (2006). *R: A Language and Environment for Statistical Computing*, Vienna: R Foundation for Statistical Computing.

Raqab, M. Z. (1998). Order statistics from the Burr type X model. *Computational Mathematical Applications* 36:111–120.

Sartawi, A., Abu-Salih, M. S. (1991). Bayesian prediction bounds for the Burr type X model. *Communications in Statistics - Theory and Methods* 20:2307–2330.

Seppala, T., Moskowitz, H., Plante, R., Tang, J. (1995). Statistical process control via the subgroup bootstrap. *Journal of Quality Technology* 27:139–153.

Surles, J. G., Padgett, W. J. (1998). Inference for $P(Y < X)$ in the Burr type X model. *Journal of Statistical Science* 7:225–238.

Surles, J. G., Padgett, W. J. (2001). Inference for reliability and stress-strength for a scaled Burr type X distribution. *Lifetime Data Analysis* 7:187–200.

Young, G. A. (1994). Bootstrap: More than a stab in the dark. *Statistical Science* 9:382–415.